DOI: 10.1534/genetics.106.063594

The *Caenorhabditis elegans rhy-1* Gene Inhibits HIF-1 Hypoxia-Inducible Factor Activity in a Negative Feedback Loop That Does Not Include *vhl-1*

Chuan Shen, Zhiyong Shao and Jo Anne Powell-Coffman[1]

Department of Genetics, Development, and Cell Biology, Iowa State University, Ames, Iowa 50011-3260

Manuscript received July 17, 2006
Accepted for publication September 5, 2006

ABSTRACT

Hypoxia-inducible factor (HIF) transcription factors implement essential changes in gene expression that enable animals to adapt to low oxygen (hypoxia). The stability of the *C. elegans* HIF-1 protein is controlled by the evolutionarily conserved EGL-9/VHL-1 pathway for oxygen-dependent degradation. Here, we describe *vhl-1*-independent pathways that attenuate HIF-1 transcriptional activity in *C. elegans*. First, the expression of HIF-1 target genes is markedly higher in *egl-9* mutants than in *vhl-1* mutants. We show that HIF-1 protein levels are similar in animals carrying strong loss-of-function mutations in either *egl-9* or *vhl-1*. We conclude that EGL-9 inhibits HIF-1 activity, as well as HIF-1 stability. Second, we identify the *rhy-1* gene and show that it acts in a novel negative feedback loop to inhibit expression of HIF-1 target genes. *rhy-1* encodes a multi-pass transmembrane protein. Although loss-of-function mutations in *rhy-1* cause relatively modest increases in *hif-1* mRNA and HIF-1 protein expression, some HIF-1 target genes are expressed at higher levels in *rhy-1* mutants than in *vhl-1* mutants. Animals lacking both *vhl-1* and *rhy-1* function have a more severe phenotype than either single mutant. Collectively, these data support models in which RHY-1 and EGL-9 function in VHL-1-independent pathway(s) to repress HIF-1 transcriptional activity.

DURING development, homeostasis, and disease, aerobic organisms must constantly adapt to changing levels of environmental oxygen. In mammals, the hypoxia-inducible factor 1 (HIF-1), a DNA-binding transcription factor, regulates many of the critical transcriptional responses to hypoxia (Lee *et al.* 2004). HIF-1 target genes play central roles in cellular and systemic responses to hypoxia, including adaptive changes in angiogenesis/vascular remodeling, erythropoiesis, glycolysis, iron metabolism, cell proliferation/survival, and extracellular-matrix metabolism (Semenza 2002; Lee *et al.* 2004). Many common human diseases, including myocardial ischemia, stroke, peripheral vascular disease, and chronic lung disease cause acute or chronic hypoxic stress (Semenza 2000). Therapies that increase HIF-1 activity may benefit patients afflicted with these and other cardiovascular illnesses. Conversely, inhibitors of HIF-1 are being employed as cancer chemotherapeutic agents, as the survival and growth of solid tumors is dependent upon adaptation to hypoxic microenvironments (Yeo *et al.* 2004). It is, therefore, of central importance to elucidate the cellular and molecular networks that regulate hypoxia-inducible factor activity.

Hypoxia-inducible factors are heterodimeric transcription factors composed of α- and β-subunits. Both subunits contain basic helix-loop-helix (bHLH) and PER-ARNT-SIM (PAS) domains that mediate dimerization and DNA binding (Wang *et al.* 1995). The β-subunit is also termed ARNT (aryl hydrocarbon receptor nuclear translocator). ARNT is broadly expressed, and it dimerizes with other bHLH-PAS proteins. The HIFα subunit is specialized for hypoxia response (Semenza 1999). There are three HIF α-genes (HIF-1α, HIF-2α, and HIF-3α) in mammals. HIF-2α and HIF-3α exhibit tissue-specific expression patterns, and HIF-1α is expressed in most cells. Mice lacking a functional HIF-1α gene die early in embryogenesis with severe vascular defects (Iyer *et al.* 1998; Ryan *et al.* 1998). HIF-1α contains two transactivation domains, which have been shown to interact with a variety of transcriptional coactivators, including CBP/p300, SRC-1, and TIF-2 (Ema *et al.* 1999; Carrero *et al.* 2000).

The EGLN family (also called the PHD or HPH family) of prolyl hydroxylases are key regulators of oxygen-dependent HIF-1 protein stability (Lando *et al.* 2003; Hirota and Semenza 2005; Kaelin 2005; Schofield and Ratcliffe 2005). In the presence of oxygen, specific proline residues (Pro-402 and Pro-564) in HIF-1α are hydroxylated by members of the EGLN family (Bruick and McKnight 2001; Epstein *et al.* 2001; Ivan *et al.* 2002). The EGLN enzymes are oxygen, iron, and 2-oxoglutarate-dependent dioxygenases (Aravind and Koonin 2001). Once hydroxylated, HIF-1α binds to the

[1]*Corresponding author:* 2108 Molecular Biology Bldg., Iowa State University, Ames, IA 50011-3260. E-mail: japc@iastate.edu

von Hippel–Lindau (pVHL) tumor suppressor, the recognition component of an E3 ubiquitin–protein ligase, and this results in ubiquitination and proteasomal degradation of HIF-1α (Cockman *et al.* 2000; Ivan *et al.* 2001; Jaakkola *et al.* 2001). Biochemical and physiological studies suggest that molecular oxygen availability may limit EGLN activity in some tissues. HIF hydroxylases are therefore thought to act as oxygen sensors that regulate HIF-1 activity (Kaelin 2005). Intensive study of HIF-1 regulation has revealed several hypoxia-dependent and -independent strategies by which cells regulate HIF translation, protein stabilization, nuclear localization, DNA-binding capacity, and transcriptional co-activator recruitment (Wenger 2002; Bardos and Ashcroft 2005; Brahimi-Horn *et al.* 2005). Recent studies also suggest that EGLN proteins may regulate HIF activity via other mechanisms, independently of their role in oxygen-dependent degradation of HIFα subunits (Ozer *et al.* 2005; To and Huang 2005).

The nematode *Caenorhabditis elegans* has proven to be a powerful model system to study evolutionarily conserved signaling pathways that regulate hypoxia response and the hypoxia-inducible factor. The *C. elegans hif-1* and *aha-1* genes are orthologous to mammalian HIFα and HIFβ subunits, respectively (Powell-Coffman *et al.* 1998; Jiang *et al.* 2001). The *hif-1* gene encodes the HIF-1 protein, and it controls most hypoxia-induced gene expression changes in *C. elegans* (Shen *et al.* 2005). *hif-1*-deficient worms are less able to survive hypoxia (Jiang *et al.* 2001; Padilla *et al.* 2002). HIF-1 protein stability is regulated by the evolutionarily conserved EGL-9/VHL-1 pathway (Epstein *et al.* 2001). *C. elegans egl-9* is orthologous to the mammalian EGLN genes, and the *C. elegans* homolog of the mammalian pVHL tumor suppressor is encoded by the *vhl-1* gene. *C. elegans* carrying loss-of-function mutations in *vhl-1* or *egl-9* express HIF-1 protein at abnormally high levels in normoxic conditions (Epstein *et al.* 2001).

In this study, we investigate *vhl-1*-independent pathways that attenuate HIF-1 activity. We present evidence that EGL-9 functions independently of VHL-1 to repress HIF-1 activity, in addition to its well-described role in the VHL-1 pathway that controls HIF-1 stability. We also identify the *rhy-1* gene, which inhibits expression of HIF-1 target genes, but has no apparent role in regulation of HIF-1 stability. Collectively, these data support models in which RHY-1 and EGL-9 function in VHL-1-independent pathway(s) to regulate HIF-1 localization or transcriptional activity.

MATERIALS AND METHODS

***C. elegans* strains and culture:** *C. elegans* were grown at 20° using standard methods (Brenner 1974). The wild-type strain was Bristol N2. CB4856 was used for single-nucleotide polymorphism (SNP) mapping. The following mutant alleles have been described previously: LGII, *unc-4*(*e120*) and *dpy-10* (*e128*); LGIII, *unc-119*(*ed3*) (Maduro and Pilgrim 1995); LGV, *egl-9*(*sa307*), *egl-9*(*n586*), *egl-9*(*n571*) (Trent *et al.* 1983; Darby *et al.* 1999), and *hif-1*(*ia04*) (Jiang *et al.* 2001); and LGX, *vhl-1*(*ok161*) (Epstein *et al.* 2001).

Genomic integration of the *nhr-57::*GFP reporter: The *nhr-57::*GFP construct was a gift from Piali Sengupta (Miyabayashi *et al.* 1999). To integrate this transgene into the genome, we employed microparticle bombardment (Praitis *et al.* 2001). The bombardment was carried out using a BioRad (Hercules, CA) Biolistic PDS/HE 1000 device, 28 in. of Hg vacuum, and 650 psi rupture disc pressure. For each bombardment, 1 μg of *unc-119* rescue plasmid pDP#MMO16b (a gift from Judith Austin) and 0.5 μg of *nhr-57::*GFP plasmid were coupled to 0.1 mg of 0.6-μm microcarrier gold beads, and the beads were bombarded onto a layer of *unc-119(ed3); vhl-1(ok161)* hermaphrodites within a 35-mm diameter circle on 100-mm NGM plates without OP50 bacteria. Worms were recovered onto "opti-gro" plates with OP50 1 hr after bombardment. Non-*unc* rescued transformants were identified 2 weeks after the bombardment. The *iaIs07* insertion [*nhr-57::*GFP; *unc-119* (+)] was mapped to LGIV using single-nucleotide polymorphisms (Wicks *et al.* 2001). The reporter then was crossed into various genetic backgrounds.

RNA interference assay: To create DNA constructs for bacteria-mediated RNA interference (RNAi), cDNAs provided by Yuji Kohara were subcloned into the L4440 double-T7 vector (Timmons and Fire 1998). When cDNAs were not available, coding sequences were PCR amplified using primers described previously (Reinke *et al.* 2000). The resulting constructs were transformed into the *Escherichia coli* strain HT115 (DE3) (Timmons and Fire 1998). RNAi analyses were performed as described previously (Kamath *et al.* 2001).

Forward genetic screen and mapping of *ia38*: The worm strain ZG119 *vhl-1*(*ok161*); *iaIs07*[*nhr-57::*GFP; *unc-119*(+)] was mutagenized with ethyl methanesulfonate (EMS) using standard methods (Jorgensen and Mango 2002). A fluorescent stereomicroscope was used to identify F_2 progeny that misexpressed the *nhr-57::*GFP reporter. Over 12,000 genomes were screened, and eight mutant strains were isolated. The *ia38* allele is described here. The *ia38* mutation was mapped by a combination of single-nucleotide polymorphisms (Wicks *et al.* 2001), deletion mapping, and three-point mapping. To create a strain suitable for mapping mutations relative to SNPs, the Hawaiian strain CB4856 was crossed to ZG119 *vhl-1*(*ok161*); *iaIs07*[*nhr-57::*GFP; *unc-119*(+)] to generate the strain ZG160. ZG160 was then backcrossed to CB4856 three times to create the strain ZG194. ZG194 is homozygous for at least 15 SNPs from the Hawaiian strain, and these were used to map mutations to specific chromosomes. Linkage of mutations to SNPs was assayed by bulk-segregated analysis (Wicks *et al.* 2001). Three-point mapping placed the *ia38* mutation between *dpy-10* and *unc-4* on LGII, at the approximate genetic map position 1.07 cM.

Generation of *rhy-1* expression constructs: To generate the *rhy-1::*GFP construct pSC09, DNA was PCR amplified using the forward primer (*Pst*I) 5′-GGCGCTGCAGCTTGGTAAG CTGACTTTCAACACG and the reverse primer (*Bam*HI) 5′-GCGGGATCCCGTGTGGCATATTGAGATGTCAAATG. The PCR product included the *rhy-1* 1.7-kb upstream promoter sequence and whole genomic sequence except the sequence for the last four codons. To construct pSC15, DNA was PCR amplified using the forward primer (*Pst*I) 5′-CACCTGCAG CAATGTATTTCAAAGAAGG and the reverse primer (*Xba*I) 5′-GTGTCTAGATGGCGATGATGACATATATGTC. The PCR product included a 1.8-kb upstream promoter sequence and +15 bp relative to the *rhy-1* translational start site. The PCR products were cloned into the green fluorescent protein (GFP) vectors pPD95.75 and pPD95.77, respectively (provided

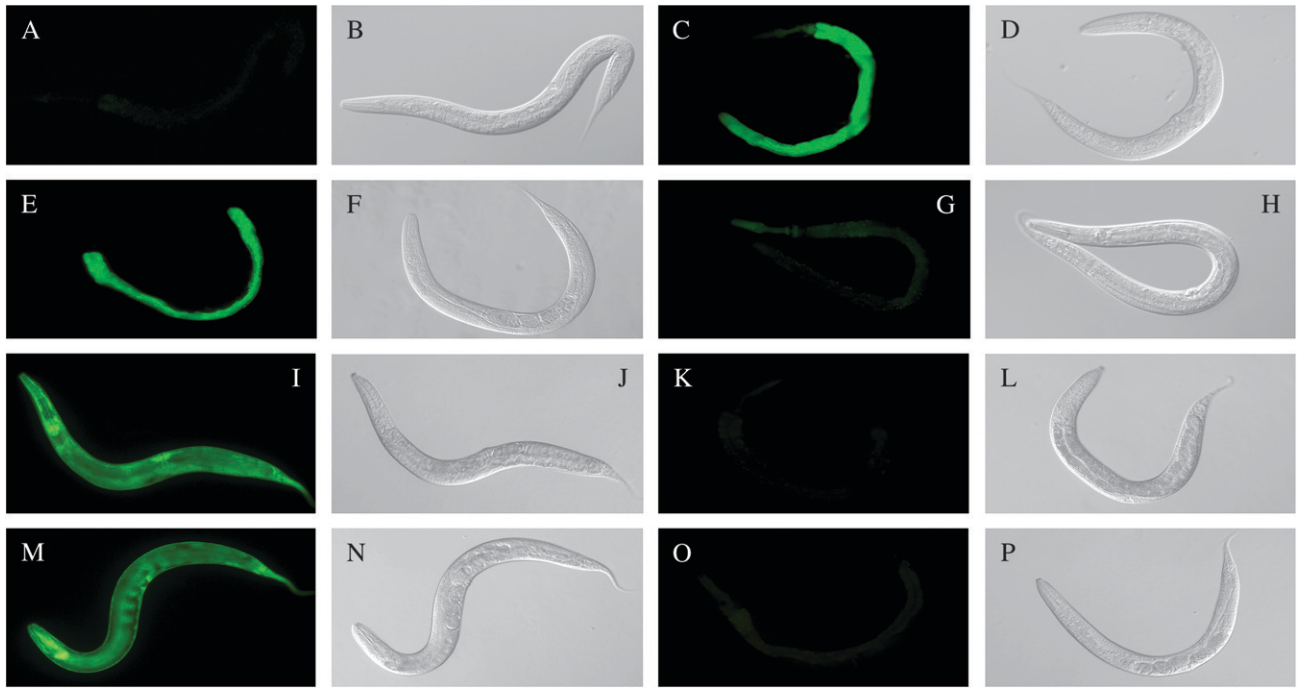

Figure 1.—*nhr-57::*GFP, a reporter of HIF-1-dependent transcription in hypoxia and in various mutant backgrounds. (A–P) *nhr-57::*GFP expression in wild-type and mutant animals, assayed by fluorescent microscopy. For each experimental condition, representative fluorescent images are paired with Nomarski images of the same animal. With the exception of C and D, all animals were incubated in room air. (A and B) Wild type. (C and D) Wild type incubated in 0.5% oxygen. (E and F) *vhl-1*(*ok161*). (G and H) *hif-1*(*ia04*); *vhl-1*(*ok161*). (I and J) *egl-9*(*sa307*). (K and L) *egl-9*(*sa307*); *hif-1(ia04*). (M and N) *rhy-1*(*ok1402*). (O and P) *rhy-1(ok1402); hif-1(ia04*).

by Andy Fire). To create transgenic animals, a solution of 20 ng/μl of pSC15 or pSC09 was injected into the gonadal syncitium, with 100 ng/μl *rol-6* (+) as a co-injection marker (Mello *et al.* 1991). Three independent transgenic lines were examined for each construct.

Western blots: L4 stage worms were collected and boiled for 5 min in 1× SDS sample buffer prepared as described (Hajdu-Cronin *et al.* 2004). The samples were loaded onto a 10% SDS–PAGE gel, size fractionated, and transferred onto Pure Nitrocellulose membrane (Osmonics, Minnetonka, MN). To detect *nhr-57::*GFP protein, 20 L4 stage worms were used in each sample. A commercially available GFP-specific mAb (Roche Diagnostics) was used in 1:1000 dilution. Secondary antibody (anti-mouse IgG and IgM from rabbit; Pierce, Rockford, IL) was used in 1:2000 dilution. To detect HIF-1 protein, 80 μg of L4 stage worm extract was loaded into each lane. Polyclonal anti-HIF-1 sera were a gift from Peter J. Ratcliffe. These antisera were produced by rabbits immunized with a glutathione-S-transferase fusion protein that included amino acids 360–498 of *C. elegans* HIF-1 (Epstein *et al.* 2001). This anti-HIF-1 was used in 1:1000 dilution, and secondary antibody (anti-rabbit IgG from goat, Jackson ImmunoResearch, West Grove, PA) was used in 1:2000 dilution. The Western blot images were analyzed by Image J software.

Real-time RT–PCR: Synchronized L4 stage worms were grown on 100-mm plates using standard methods. Total RNA was isolated using Trizol reagent. RNA samples were treated by the TURBO DNA-free kit (Ambion, Austin, TX) to remove the DNA contamination. One microgram of total RNA from each sample was converted to complementary DNA using the anchored oligo(dT) primer according to the manufacturer's protocol (EndoFree RT kit, Ambion). Fifty nanograms of total RNA from each sample was used for each real-time RT–PCR reaction using the Full Velocity SYBR Green QPCR Master Mix kit (Stratagene, La Jolla, CA). Quantitative RT–PCR was performed using the Stratagene Mx4000 multiplex PCR system. The specific primers for K10H10.2, F22B5.4, and *inf-1* were designed and synthesized by Integrated DNA Technologies. The standard curve method was used to analyze the expression levels. *inf-1* is not regulated by hypoxia (Shen *et al.* 2005) and was used as a control. The experiments were repeated in triplicate.

RESULTS

To develop a visual assay for HIF-1 transcriptional activity, we examined the expression of reporter constructs in which the expression of GFP was controlled by regulatory sequences from HIF-1 target genes (Shen *et al.* 2005). Of the reporters that we assayed, *nhr-57::*GFP (Miyabayashi *et al.* 1999) was the most reliable reporter of HIF-1 function, and we used microparticle bombardment to integrate the *nhr-57*::GFP into the *C. elegans* genome. This reporter was expressed at very low levels in wild-type animals in room air (Figure 1A). Hypoxia treatment increased *nhr-57::*GFP levels markedly (Figure 1C). Prior studies have shown that mutants defective for *vhl-1* express HIF-1 protein and *nhr-57* mRNA at constitutively high levels (Figure 2A; Epstein *et al.* 2001; Bishop *et al.* 2004; Shen *et al.* 2005). We determined that the *nhr-57::*GFP reporter was expressed at high levels in *vhl-1* mutants and that *nhr-57::*GFP

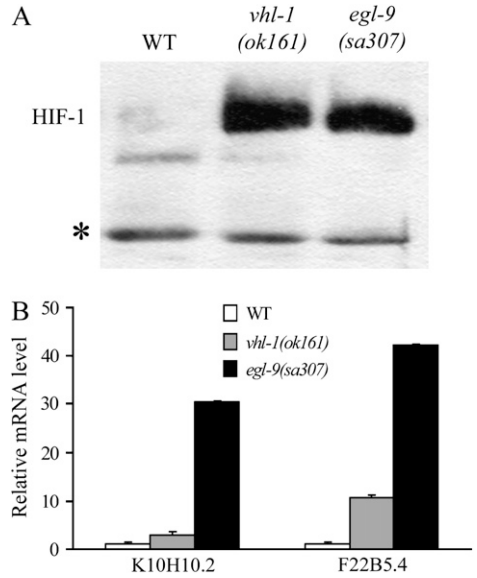

Figure 2.—EGL-9 acts via VHL-1-dependent and VHL-1-independent pathways to regulate HIF-1. (A) The levels of endogenous HIF-1 protein were assayed in wild type N2, *vhl-1*(*ok161*), and *egl-9(sa307)* L4 stage animals. The asterisk indicates an unidentified protein that is recognized by the HIF-1 antibody, but is also present in *hif-1(ia04)* animals, which have a large deletion in the *hif-1* gene. (B) Real-time RT–PCR was used to quantitate mRNA levels of HIF-1 target genes in wild-type and mutant worms. The graph depicts average values from three independent experiments, and the error bars represent the mean standard error.

expression required *hif-1* function (Figure 1, E and G). Thus, *nhr-57::*GFP was a useful visual assay for HIF-1 activity.

***vhl-1*-independent functions of *egl-9*:** We were intrigued to find that *egl-9*-deficient animals expressed *nhr-57::*GFP at higher levels than did *vhl-1* mutants. Both *egl-9*(*sa307*) and *vhl-1*(*ok161*) are strong loss-of-function alleles. While expression of the reporter was strongly enriched in the intestine of *vhl-1*(*ok161*) animals (Figure 1E), *nhr-57::*GFP fluorescence was also visible in the hypodermis and pharynx of *egl-9*(*sa307*) mutants (Figure 1I). A similar pattern and level of reporter gene expression was observed with the *egl-9*(*n586*) and *egl-9(n571)* loss-of-function alleles (data not shown). This observation was consistent with an independent, concurrent study in which *nhr-57* mRNA levels were found to be higher in *egl-9* mutant animals compared to *vhl-1* mutants (Bishop *et al.* 2004). To further characterize the *egl-9* mutant phenotype, we employed real-time RT–PCR to quantitate the expression K10H10.2 and F22B5.4 mRNAs. In prior studies, we had established that these two genes were induced by hypoxia in a *hif-1*-dependent manner (Shen *et al.* 2005). As shown in Figure 2B, loss-of-function mutations in *vhl-1* or *egl-9* caused F22B5.4 mRNA to be overexpressed 11-fold and 42-fold, respectively. A similar pattern was seen with K10H10.2 mRNA expression. *vhl-1*-deficient worms expressed K10H10.2 mRNA at levels 3-fold higher than found in wild type. By comparison, *egl-9(sa307*) mutants overexpressed K10H10.2 mRNA 30-fold, relative to wild type. This difference between the *egl-9(sa307)* and *vhl-1*(*ok161*) phenotypes was highly significant (Figure 2B, $P < 0.00001$). These analyses provide strong genetic evidence that EGL-9 acts through both VHL-1-dependent and VHL-1-independent pathways to antagonize HIF-1.

We considered the possible mechanisms by which EGL-9 might decrease expression of HIF-1 target genes independently of VHL-1. One possibility was that once HIF-1 was hydroxylated by EGL-9, it was targeted for degradation by an E3 ligase other than VHL-1. This model predicted that HIF-1 protein levels would be significantly higher in *egl-9* mutant animals compared to *vhl-1* mutant animals. We employed immunoblots to test this hypothesis (Figure 2A). HIF-1 protein was expressed at similar levels in *vhl-1*(*ok161*) and *egl-9(sa307*) animals (averaging 4.8-fold and 4.5-fold greater than wild type, respectively). We also examined the expression of a transgene in which HIF-1 protein was tagged with GFP (Jiang *et al.* 2001). Strong loss-of-function mutations in *vhl-1* or *egl-9* resulted in similar levels of HIF-1::GFP expression (data not shown). Thus, EGL-9 and VHL-1 act in concert to regulate HIF-1 protein levels, and EGL-9 also functions via a separate VHL-1-independent pathway to inhibit HIF-1 activity.

***rhy-1*, an integral membrane protein that inhibits HIF-1 function:** To further define the *vhl-1*-independent pathway(s) by which *egl-9* and other genes regulated HIF-1 activity, we employed two experimental strategies. First, we initiated a forward genetic screen to identify mutations that caused an *nhr-57::*GFP expression pattern similar to that seen in *egl-9* mutants (described below). Second, we used bacterially mediated RNAi to test the hypothesis that some HIF-1 target genes might be negative regulators of HIF-1 function. Prior studies had shown that *C. elegans* EGL-9 and the mammalian EGLN1/PHD2 and EGLN3/PHD3 genes acted in negative feedback loops to attenuate HIF activity (D'Angelo *et al.* 2003; Aprelikova *et al.* 2004; Bishop *et al.* 2004; Shen *et al.* 2005). Similarly, the mammalian CITED2 gene has been shown to be induced by HIF-1 and to feed back to block binding of HIF-1α to CBP/p300 (Bhattacharya *et al.* 1999). In a previous study, we identified 63 *C. elegans* genes that were induced by hypoxia in a HIF-1-dependent manner (Shen *et al.* 2005), and we will refer to these here as HIF-1 target genes. To test the hypothesis that some genes activated by *C. elegans* HIF-1 functioned to limit HIF-1 activity, we used bacterially mediated RNAi (Kamath *et al.* 2001) to reduce expression of 9 HIF-1 target genes. RNAi for W07A12.7 increased and expanded *nhr-57::*GFP expression. This phenotype was similar to that exhibited by *egl-9* mutant worms (data not shown; described further below). On the basis of the characterization of the

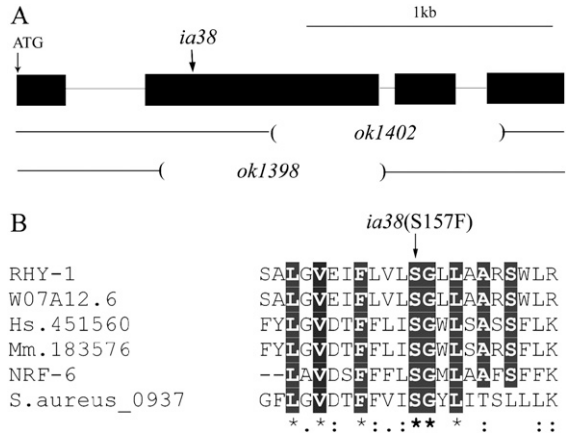

FIGURE 3.—*rhy-1* gene and mutant alleles. (A) Diagram of the *rhy-1*/W07A12.7 genomic region. Exons are indicated by boxes. Arrows indicate the positions of the start codon ATG and the position of the *ia38* S157F point mutation. The endpoints of the *ok1402* and *ok1398* deletions are represented by parentheses. (B) The *ia38* mutation is in a highly conserved region. RHY-1 is aligned with five other members of the gene family. Asterisks indicate amino acid identities. The arrow indicates the position of the *ia38* S157F point mutation. The NCBI reference numbers for the mammalian and bacterial sequences are Unigene Hs.451560, Unigene Mm.183576, and accession no. Q6GIB3. The *C. elegans* genes *rhy-1*, W07A12.6, and *nrf-6* are described at http://www.wormbase.org.

loss-of-function phenotype, we named the W07A12.7 gene *rhy-1* (*r*egulator of *hy*poxia-inducible factor).

Concurrently, we conducted a forward genetic screen for EMS-induced mutations that increased the expression of the *nhr-57::*GFP reporter in *vhl-1(ok161)* animals. Here, we describe the *ia38* allele. Animals that were homozygous for the *ia38* mutation exhibited a phenotype similar to that caused by *rhy-1* RNAi. We mapped *ia38* to a 1.1-cM genomic interval between *dpy-10* and *unc-4* on chromosome II. The mutant phenotype and genomic location suggested that the *ia38* mutation might be in the *rhy-1* gene. In support of this hypothesis, we determined that an extrachromosomal array containing a wild-type copy of *rhy-1* was able to rescue the *ia38* phenotype. We sequenced the *rhy-1* gene in *ia38* mutants and determined that *ia38* animals contained a missense mutation that changed a conserved serine to phenylalanine (the position of Ser157 is indicated by an arrow in Figure 3, A and B). At our request, the *C. elegans* Knockout Consortium isolated two deletion mutations in *rhy-1*, which are diagrammed in Figure 3A. The *ok1402* lesion deletes the region that encodes amino acids 246–429 (>36% of the predicted *rhy-1* coding sequence). The *rhy-1(ok1398)* mutation deletes the genomic region encoding amino acids 86–337. Animals that are homozygous for either *ok1398* or *ok1402* overexpress the *nhr-57::*GFP reporter, and this phenotype is suppressed by a strong loss-of-function mutation in *hif-1* (Figure 1, M and O; data not shown). The deletion mutations fail to complement the *ia38* allele. We conclude that *ia38* is a mutation in the *rhy-1* gene. The three *rhy-1* alleles (*ia38*, *ok1402*, and *ok1398*) have similar phenotypes, as assessed by morphological defects and *nhr-57::*GFP expression patterns.

The RHY-1 protein is predicted to be an integral membrane protein with up to 11 membrane-spanning domains and an acyltransferase-3 domain (previously annotated as domain of unknown function 33). This large motif is found in a range of bacterial enzymes that catalyze the transfer of acyl groups, other than aminoacyl, from one compound to another. The molecular functions of metazoan proteins belonging to this gene family are unknown. The serine residue mutated in the *rhy-1 (ia38)* allele is highly conserved. Figure 3B is an alignment of the amino acids surrounding this serine residue for related worm, human, mouse, and bacterial proteins. Computational analyses suggest that RHY-1 is localized to the plasma membrane or to the endoplasmic reticulum (http://psort.nibb.ac.jp).

There are 63 other genes in the *C. elegans* genome that contain acyltransferase-3 domains, including *nrf-6*, *ndg-4*, and W07A12.6. Loss-of-function mutations in *ndg-4* or *nrf-6* cause defects in yolk lipoprotein export from intestinal cells and confer resistance to fluoxetine (CHOY and THOMAS 1999; CHOY *et al.* 2006). *nrf-6* loss-of-function mutants do not mis-express the *nhr-57::GFP* reporter (data not shown). The W07A12.6 gene is adjacent to *rhy-1*, and it is predicted to encode a protein with 78% sequence identity to the *rhy-1* gene product. W07A12.6 mRNA is induced by hypoxia (SHEN *et al.* 2005). We were not able to deplete W07A12.6 mRNA by RNAi without also targeting *rhy-1*, due to the high level of sequence similarity between the two genes (data not shown).

Comparison of *rhy-1* and *egl-9* loss-of-function phenotypes: The morphological defects in *rhy-1*(*ok1402)* and *egl-9*(*sa307)* mutants were similar, and the two mutations resulted in comparable patterns of *nhr-57::*GFP expression (Figure 1, I and M). Others have shown that the *egl-9* egg-laying defect is suppressed by a strong loss-of-function mutation in *hif-1* (BISHOP *et al.* 2004). Thus, the morphological defects in *egl-9*-deficient worms are due, in large part, to abnormally high levels of HIF-1 function. Animals that were homozygous for any of the three *rhy-1* alleles exhibited egg-laying defects and were slightly dumpy. These morphological defects were suppressed by the *hif-1*(*ia04)* deletion allele. The *rhy-1*(*ok1402); hif-1*(*ia04)* double mutants produced an average of only 21 self-progeny/hermaphrodite (of 45 broods scored). By comparison, the *rhy-1*(*ok1402)* mutation reduced the brood size much less dramatically, to 188 self-progeny. Wild-type hermaphrodites and *hif-1*(*ia04)* single mutants produced 251 and 253 self-progeny, respectively (of 20 broods assayed). The low fecundity of *rhy-1*(*ok1402); hif-1*(*ia04)* hermaphrodites was rescued by mating to wild-type males. This suggested

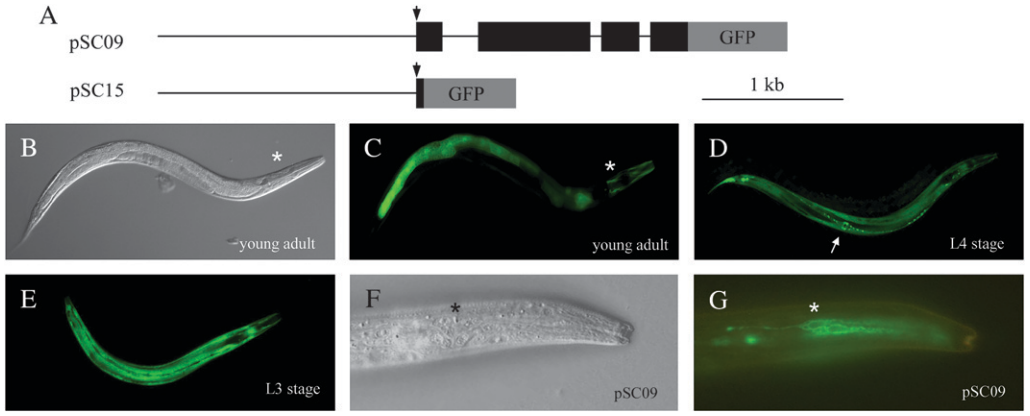

Figure 4.—RHY-1::GFP expression pattern. (A) Structures of two reporters, in which GFP is fused to *rhy-1* regulatory sequences. pSC09 includes the entire *rhy-1* coding region and can rescue the *rhy-1 ia38*, *ok1402*, and *ok1398* mutant phenotypes. Boxes represent exons. (B–G) *C. elegans* carrying the pSC15 (B–E) and pSC09 (F and G) reporter constructs. Anterior is to the right. (B and C). Nomarski image (B) and fluorescent image (C) of a young adult hermaphrodite carrying the pSC15 reporter. GFP is strongly visible in the intestine and in certain head sensory neurons. (D) An L4 stage hermaphrodite. GFP is visible in hypodermal cells, the vulva (indicated by the arrow), and cells of the ventral nerve cord. (E) An L3 stage larva with strong hypodermal GFP fluorescence. (F and G) Nomarski image (F) and fluorescent image (G) of pSC09 expression in the head of an L2 stage animal.

that *rhy-1*(*ok1402*); *hif-1*(*ia04*) double-mutant hermaphrodites produced low numbers of functional sperm. In contrast, *egl-9*(*sa307*); *hif-1*(*ia04*) double mutants had normal brood sizes. These analyses suggest that while both *rhy-1* and *egl-9* act to inhibit expression of certain HIF-1 target genes, *rhy-1* has roles in sperm development that do not require *egl-9* function.

RHY-1 expression pattern: The *rhy-1*-defective phenotypes suggested that *rhy-1* function was required in multiple tissues. To gain further insight into RHY-1 function, we created RHY-1::GFP reporter constructs and assayed their expression patterns. The pSC15 *rhy-1::*GFP fusion included only five *rhy-1* codons (Figure 4A). This reporter was expressed in several tissues. In adults, this reporter was expressed highly in the intestine and in certain sensory neurons in the head and at lower levels in body-wall muscles and socket cells (Figure 4C). During the last larval stage, GFP was visible in the vulva, in cells in the ventral nerve cord, and in cells in the tail (Figure 4D). Larval stage animals expressed pSC15 at high levels in the hypodermis (Figure 4E). Hypoxia treatment increased the levels of reporter gene expression (data not shown). Prior studies have localized *egl-9::*GFP to pharyngeal muscle, body-wall muscle, vulval muscles, and sensory neurons of the head and tail (Darby *et al.* 1999). Thus, the expression patterns of *rhy-1::*GFP and *egl-9::*GFP partially overlap.

The pSC09 construct contained the predicted *rhy-1* coding sequences, the three *rhy-1* introns, and 1.7 kb of sequence 5′ to the start codon (Figure 4A). This fusion gene was expressed at low levels, but it rescued all three of the *rhy-1* mutant alleles, as assayed by *nhr-57::* GFP expression (data not shown). In animals carrying pSC09, GFP expression was perinuclear and was visible in intracellular reticular patterns. This was consistent with the prediction that RHY-1 is localized to the endoplasmic reticulum.

RHY-1 inhibits HIF-1 activity via a VHL-1-independent pathway: As shown in Figure 1 and in Figure 5C, *rhy-1*(*ok1402*) and *egl-9*(*sa307*) animals expressed *nhr-57::*GFP at high levels, relative to *vhl-1*(*ok161*) animals. To confirm that *rhy-1* inhibited the expression of HIF-1 target genes other than *nhr-57::*GFP, we assayed expression of two endogenous mRNAs, K10H10.2 and F22B5.4, by real-time RT–PCR. Mutation of *rhy-1* significantly increased the expression of both genes ($P < 0.0001$ and $P < 0.01$, respectively), and this effect was suppressed by the *hif-1*(*ia04*) deletion mutation (Figure 5, A and B). Expression of K10H10.2 and F22B5.4 mRNAs was higher in *rhy-1*(*ok1402*); *vhl-1*(*ok161*) double mutants than in either single mutant (Figure 5, A and B). Double mutants also expressed *nhr-57::*GFP protein at significantly higher levels than did either single mutant (Figure 5C, $P < 0.05$). Interestingly, the level of F22B5.4 mRNA in *rhy-1* and *vhl-1* mutants was similar, but K10H10.2 mRNA was expressed at a significantly higher level in *rhy-1* mutants (Figure 5A, $P < 0.00001$). This suggests that the relative importance of the VHL-1 and RHY-1 pathways may vary between cell types and promoters.

To address whether RHY-1 regulates HIF-1 expression, HIF-1 activity, or both, we assayed *hif-1* mRNA and HIF-1 protein levels. The *rhy-1*(*ok1402*) mutation resulted in a slight increase in *hif-1* mRNA levels (1.8-fold) (Figure 5D) and HIF-1 protein (2.2-fold) (Figure 5E). By comparison, HIF-1 protein levels in *vhl-1*(*ok161*) and *egl-9(sa309)* animals were 4.8-fold and 4.5-fold greater than in wild-type animals (Figure 5E), while *hif-1* mRNA levels were not changed (Figure 5D). This is consistent with a model in which RHY-1 has a minor effect on HIF-1 protein expression and functions primarily in a VHL-1-independent pathway to limit HIF-1 function.

If EGL-9 and RHY-1 acted in distinct pathways, then we would expect that the expression of HIF-1 target genes might be higher in the double mutant than in

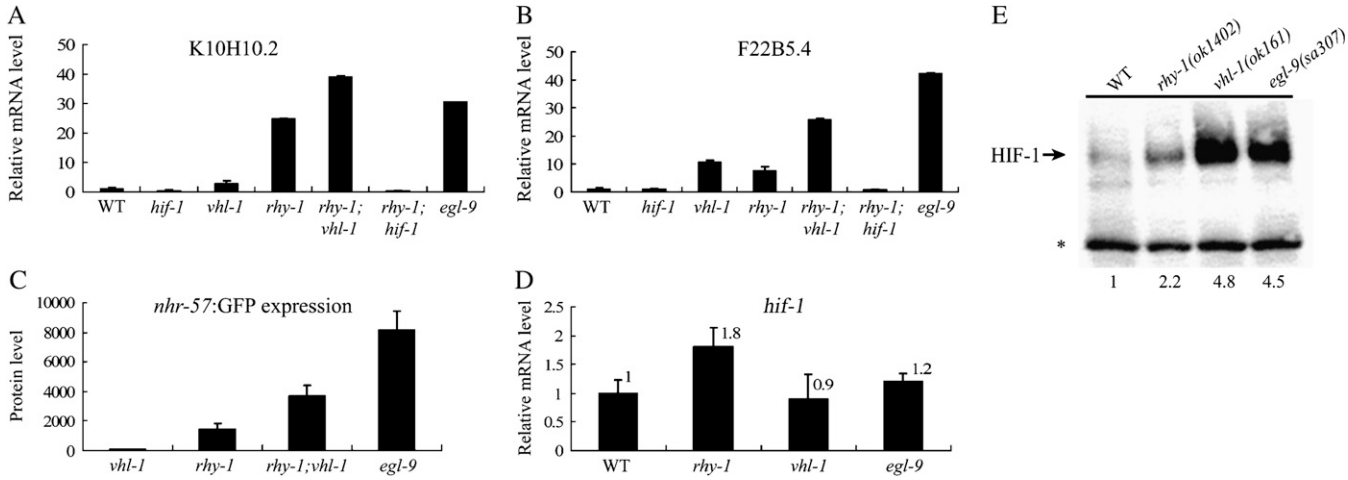

FIGURE 5.—RHY-1 has VHL-1-independent functions. (A and B) Expression of two HIF-1 target genes in various mutants. K10H10.2 and F22B5.4 mRNA levels were quantitated by real-time RT–PCR in three independent experiments. (C) Relative levels of *nhr-57::*GFP as determined by immunoblots. (D) *hif-1* mRNA levels were assessed by real-time RT–PCR. Numbers indicate the relative mRNA levels compared with wild-type worms. The following alleles were used for the above studies: *rhy-1(ok1402)*, *egl-9(sa307)*, *hif-1(ia04)*, and *vhl-1(ok161)*. Error bars represent the mean standard error from three independent experiments. (E) Protein blots probed with HIF-1 antisera. The position of HIF-1 is indicated by the arrow. The relative expression levels of HIF-1 are indicated below each lane. These are average values from three independent experiments. The asterisk indicates an unidentified protein that is recognized by the HIF-1 antibody, but is also present in *hif-1(ia04)* worms, which carry a large deletion in *hif-1*.

either single mutant. To test this, we assayed the expression of *nhr-57::*GFP protein, K10H102 mRNA, and F22B5.4 mRNA in *rhy-1(ok1402)*, *egl-9(sa307)* and double-mutant animals. For all three genes assayed, expression in *rhy-1(ok1402); egl-9(sa307)* double mutants was not enhanced relative to expression in *egl-9* single mutants (Figure 6, A and B). While not conclusive, these data leave open the possibility that RHY-1 and EGL-9 function in the same pathway.

DISCUSSION

The transcription factor HIF is a central regulator of physiological and pathological adaptation to hypoxia. The regulation of HIF activity occurs at the multiple levels, and the cellular networks that control HIF include negative and positive interactions (CHUN *et al.* 2002; DERY *et al.* 2005). We have employed genetic strategies to further understand the regulatory circuits that control transcriptional responses to hypoxia.

Dual functions for EGL-9: We conclude that EGL-9 inhibits HIF-1 function via VHL-1-independent pathway(s), in addition to its well-described role in controlling HIF-1 stabilization. The EGL-9/VHL-1 pathway has been studied intensively. EGL-9 hydroxylates HIF-1 in an oxygen-dependent manner. This modification results in VHL-1 binding and subsequent ubiquitination and proteasomal degradation of HIF-1 (EPSTEIN *et al.* 2001). In this study, we show that *egl-9* mutants express HIF-1 target genes at higher levels than do *vhl-1* mutants. Moreover, we show that this difference in HIF-1 function is not attributable to differences in HIF-1 protein levels. These results provide strong support for models in which EGL-9 represses the activity of HIF-1 protein.

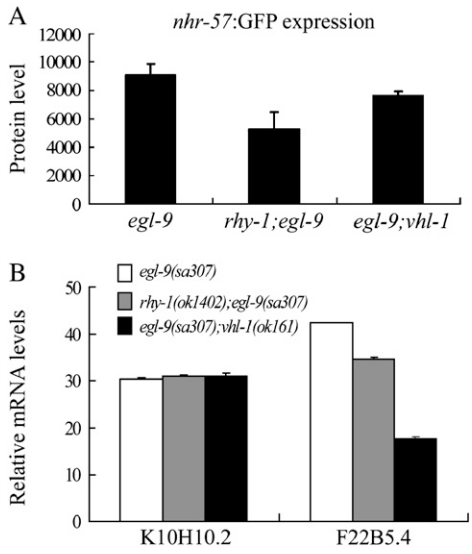

FIGURE 6.—The *egl-9* mutant phenotype, as assayed by expression of HIF-1 target genes, is not increased in severity by additional mutations in *vhl-1* or *rhy-1*. (A) *nhr-57::*GFP protein levels assayed on immunoblots. Total protein from 20 L4 stage animals was loaded into each lane. (B) Relative expression of the HIF-1 target genes K10H10.2 and F22B5.4, as determined by real-time RT–PCR. The following alleles were used: *rhy-1(ok1402)*, *egl-9(sa307)*, and *vhl-1(ok161)*. In each case, an average of three independent experiments and the mean standard error are shown.

Two recent studies in mammalian cell lines provide further insight into mechanisms by which EGLN proteins might regulate HIF activity independently of VHL. First, the candidate tumor suppressor ING4 was shown to form a complex with EGLN1/HPH-2. Additionally, EGLN1/HPH-2 and ING4 were shown to associate with DNA-binding sites for HIF (Ozer *et al.* 2005). This study provides support for a model in which HPH-2/EGLN1 recruits ING4 and transcriptional repressors to the HIF complex, thereby inhibiting the expression of HIF target genes. Another group has presented further evidence that EGLN1 inhibits HIF-1α transcriptional activity independently of the VHL pathway that regulates HIF-1α protein stability (To and Huang 2005). When considered with these studies, the *C. elegans* data are consistent with the following model: EGL-9 binds HIF-1 at the conserved LXXLAP motif in the ODD domain. When the oxygen concentration is sufficiently high, EGL-9 hydroxylates HIF-1, resulting in binding to VHL-1 and subsequent degradation of HIF-1 (Epstein *et al.* 2001). EGL-9 also binds HIF-1 in the nucleus, and EGL-9 recruits certain transcriptional repressors to the regulatory regions of HIF-1 target genes. Clearly, many aspects of this model remain to be tested. However, it is interesting to note that *C. elegans* EGL-9 and mammalian EGLN1 each include an N-terminal MYND-type zinc-finger domain and that this protein motif is present in certain transcriptional repressors (Lutterbach *et al.* 1998; Masselink and Bernards 2000; Gottlieb *et al.* 2002).

RHY-1: Under hypoxic conditions *rhy-1* mRNA expression is induced by HIF-1, and RHY-1 feeds back to attenuate HIF-1 activity. In this report, we demonstrate that RHY-1 inhibits expression of HIF-1 target genes via a mechanism that is distinct from the VHL-1-mediated pathway that controls HIF-1 protein levels.

The molecular function(s) of RHY-1 are unknown. The RHY-1 protein is predicted to include up to 11 membrane-spanning domains, and it appears to be localized to the endoplasmic reticulum or to the plasma membrane. Analysis of the RHY-1 sequence reveals a single motif that may be informative to its biochemical function: the acyltransferase-3 domain. The acyltransferase-3 domain arose before the evolution of the hypoxia-inducible factor, and it is predicted to catalyze the transfer of acyl groups, other than amino-acyl, from one compound to another. Thus, RHY-1 may have roles in the synthesis, metabolism, or transport of bioactive lipids that modulate HIF-1 activity. Interestingly, while the *C. elegans* genome contains 64 genes with acyltransferase-3 motifs, the human, mouse, and Drosophila genomes each contain only one member of this gene family. It will be interesting to elucidate how RHY-1 modulates HIF-1 regulatory circuits and to determine whether the mammalian acyltransferase-3 gene family members have roles in hypoxia response.

There are at least three alternative models to describe how RHY-1 might attenuate expression of HIF-1 target genes. The simplest model is that RHY-1 binds HIF-1 directly and inhibits nuclear translocation of the transcription factor. A second possibility is that RHY-1 has a role in the metabolism or transport of bioactive lipids, which then control HIF-1 localization or transcriptional activity. This model would be consistent with the critical role of Ser157. The serine residue that is mutated in the *rhy-1(ia38)* allele is predicted to be in the second transmembrane domain of RHY-1 and could be involved in putative transporter functions for RHY-1. In further support of this model, the *C. elegans* NRF-6 acyltransferase-3 protein has been shown to interact with NRF-5, a predicted lipid-binding protein (Choy *et al.* 2006). Third, RHY-1 might function indirectly by modulating other cellular processes that ultimately control HIF-1 function. Two of these models invoke as-of-yet-unidentified sensors of lipids or other molecules regulated by RHY-1, and these sensors are postulated to control HIF-1 function. Clearly, it will be informative to identify other genes that interact with RHY-1 to control HIF-1. RHY-1 has an essential role in a negative feedback loop that limits expression of HIF-1 target genes, and we favor models in which regulating HIF-1 is a primary function for RHY-1.

Both EGL-9 and RHY-1 act in negative feedback loops to limit transcription of HIF-1 target genes, but it is not yet clear whether these two proteins act in concert. Interestingly, the repressive function of EGL-9 appears to be greater than that of RHY-1. As described above, EGL-9 might recruit transcriptional repressors to the HIF-1 complex. If this is true, then RHY-1 might regulate the localization or association of HIF-1, EGL-9, and putative repressors.

When considering these models, it is interesting to note that hypoxia treatment resulted in a *nhr-57*::GFP expression pattern that was similar to that seen in *vhl-1* mutants, but less intense than that seen in *rhy-1*- or *egl-9*-defective animals (see Figure 1). Prior studies have established that hypoxia inhibits EGL-9 enzymatic activity and VHL-1-dependent degradation of HIF-1 (Epstein *et al.* 2001). However, it is possible that EGL-9 oxygenase activity is not required for the VHL-1-independent functions of EGL-9. Further studies will address these intriguing hypotheses, as they will ultimately inform our understanding of the regulatory circuits that control the hypoxia-inducible factor during development, homeostasis, and disease.

We thank Piali Sengupta, Peter Ratcliffe, Ann Rose, and Andy Fire for providing plasmids or antibodies used in these studies. We are grateful to Abhijeet Shah, Kelly Gillette, and Mae Young for their roles in isolating and mapping the *rhy-1(ia38)* allele. Mutant strains were obtained from the Caenorhabditis Genetics Center, which is supported by the National Institutes of Health National Center for Research Resources. An American Heart Association Established Investigator award to J.A.P.C. provided funding for this work.

LITERATURE CITED

Aprelikova, O., G. V. Chandramouli, M. Wood, J. R. Vasselli, J. Riss *et al.*, 2004 Regulation of HIF prolyl hydroxylases by hypoxia-inducible factors. J. Cell. Biochem. **92:** 491–501.

Aravind, L., and E. V. Koonin, 2001 The DNA-repair protein AlkB, EGL-9, and leprecan define new families of 2-oxoglutarate- and iron-dependent dioxygenases. Genome Biol. **2:** RESEARCH0007.

Bardos, J. I., and M. Ashcroft, 2005 Negative and positive regulation of HIF-1: a complex network. Biochim. Biophys. Acta **1755:** 107–120.

Bhattacharya, S., C. L. Michels, M. K. Leung, Z. P. Arany, A. L. Kung *et al.*, 1999 Functional role of p35srj, a novel p300/CBP binding protein, during transactivation by HIF-1. Genes Dev. **13:** 64–75.

Bishop, T., K. W. Lau, A. C. Epstein, S. K. Kim, M. Jiang *et al.*, 2004 Genetic analysis of pathways regulated by the von Hippel-Lindau tumor suppressor in *Caenorhabditis elegans*. PLoS Biol. **2:** e289.

Brahimi-Horn, C., N. Mazure and J. Pouyssegur, 2005 Signalling via the hypoxia-inducible factor-1alpha requires multiple post-translational modifications. Cell. Signal. **17:** 1–9.

Brenner, S., 1974 The genetics of *Caenorhabditis elegans*. Genetics **77:** 71–94.

Bruick, R. K., and S. L. McKnight, 2001 A conserved family of prolyl-4-hydroxylases that modify HIF. Science **294:** 1337–1340.

Carrero, P., K. Okamoto, P. Coumailleau, S. O'Brien, H. Tanaka *et al.*, 2000 Redox-regulated recruitment of the transcriptional coactivators CREB-binding protein and SRC-1 to hypoxia-inducible factor 1alpha. Mol. Cell. Biol. **20:** 402–415.

Choy, R. K., and J. H. Thomas, 1999 Fluoxetine-resistant mutants in *C. elegans* define a novel family of transmembrane proteins. Mol. Cell **4:** 143–152.

Choy, R. K., J. M. Kemner and J. H. Thomas, 2006 Fluoxetine-resistance genes in *Caenorhabditis elegans* function in the intestine and may act in drug transport. Genetics **172:** 885–892.

Chun, Y. S., M. S. Kim and J. W. Park, 2002 Oxygen-dependent and -independent regulation of HIF-1alpha. J. Korean Med. Sci. **17:** 581–588.

Cockman, M. E., N. Masson, D. R. Mole, P. Jaakkola, G. W. Chang *et al.*, 2000 Hypoxia inducible factor-alpha binding and ubiquitylation by the von Hippel-Lindau tumor suppressor protein. J. Biol. Chem. **275:** 25733–25741.

D'Angelo, G., E. Duplan, N. Boyer, P. Vigne and C. Frelin, 2003 Hypoxia up-regulates prolyl hydroxylase activity: a feedback mechanism that limits HIF-1 responses during reoxygenation. J. Biol. Chem. **278:** 38183–38187.

Darby, C., C. L. Cosma, J. H. Thomas and C. Manoil, 1999 Lethal paralysis of *Caenorhabditis elegans* by *Pseudomonas aeruginosa*. Proc. Natl. Acad. Sci. USA **96:** 15202–15207.

Dery, M. A., M. D. Michaud and D. E. Richard, 2005 Hypoxia-inducible factor 1: regulation by hypoxic and non-hypoxic activators. Int. J. Biochem. Cell Biol. **37:** 535–540.

Ema, M., K. Hirota, J. Mimura, H. Abe, J. Yodoi *et al.*, 1999 Molecular mechanisms of transcription activation by HLF and HIF1alpha in response to hypoxia: their stabilization and redox signal-induced interaction with CBP/p300. EMBO J. **18:** 1905–1914.

Epstein, A. C., J. M. Gleadle, L. A. McNeill, K. S. Hewitson, J. O'Rourke *et al.*, 2001 *C. elegans* EGL-9 and mammalian homologs define a family of dioxygenases that regulate HIF by prolyl hydroxylation. Cell **107:** 43–54.

Gottlieb, P. D., S. A. Pierce, R. J. Sims, H. Yamagishi, E. K. Weihe *et al.*, 2002 Bop encodes a muscle-restricted protein containing MYND and SET domains and is essential for cardiac differentiation and morphogenesis. Nat. Genet. **31:** 25–32.

Hajdu-Cronin, Y. M., W. J. Chen and P. W. Sternberg, 2004 The L-type cyclin CYL-1 and the heat-shock-factor HSF-1 are required for heat-shock-induced protein expression in *Caenorhabditis elegans*. Genetics **168:** 1937–1949.

Hirota, K., and G. L. Semenza, 2005 Regulation of hypoxia-inducible factor 1 by prolyl and asparaginyl hydroxylases. Biochem. Biophys. Res. Commun. **338:** 610–616.

Ivan, M., K. Kondo, H. Yang, W. Kim, J. Valiando *et al.*, 2001 HIFalpha targeted for VHL-mediated destruction by proline hydroxylation: implications for O2 sensing. Science **292:** 464–468.

Ivan, M., T. Haberberger, D. C. Gervasi, K. S. Michelson, V. Gunzler *et al.*, 2002 Biochemical purification and pharmacological inhibition of a mammalian prolyl hydroxylase acting on hypoxia-inducible factor. Proc. Natl. Acad. Sci. USA **99:** 13459–13464.

Iyer, N. V., L. E. Kotch, F. Agani, S. W. Leung, E. Laughner *et al.*, 1998 Cellular and developmental control of O2 homeostasis by hypoxia-inducible factor 1 alpha. Genes Dev. **12:** 149–162.

Jaakkola, P., D. R. Mole, Y. M. Tian, M. I. Wilson, J. Gielbert *et al.*, 2001 Targeting of HIF-alpha to the von Hippel-Lindau ubiquitylation complex by O2-regulated prolyl hydroxylation. Science **292:** 468–472.

Jiang, H., R. Guo and J. A. Powell-Coffman, 2001 The *Caenorhabditis elegans hif-1* gene encodes a bHLH-PAS protein that is required for adaptation to hypoxia. Proc. Natl. Acad. Sci. USA **98:** 7916–7921.

Jorgensen, E. M., and S. E. Mango, 2002 The art and design of genetic screens: *Caenorhabditis elegans*. Nat. Rev. Genet. **3:** 356–369.

Kaelin, W. G., 2005 Proline hydroxylation and gene expression. Annu. Rev. Biochem. **74:** 115–128.

Kamath, R. S., M. Martinez-Campos, P. Zipperlen, A. G. Fraser and J. Ahringer, 2001 Effectiveness of specific RNA-mediated interference through ingested double-stranded RNA in *Caenorhabditis elegans*. Genome Biol. **2:** RESEARCH0002.

Lando, D., J. J. Gorman, M. L. Whitelaw and D. J. Peet, 2003 Oxygen-dependent regulation of hypoxia-inducible factors by prolyl and asparaginyl hydroxylation. Eur. J. Biochem. **270:** 781–790.

Lee, J. W., S. H. Bae, J. W. Jeong, S. H. Kim and K. W. Kim, 2004 Hypoxia-inducible factor (HIF-1) alpha: its protein stability and biological functions. Exp. Mol. Med. **36:** 1–12.

Lutterbach, B., D. Sun, J. Schuetz and S. W. Hiebert, 1998 The MYND motif is required for repression of basal transcription from the multidrug resistance 1 promoter by the t(8;21) fusion protein. Mol. Cell. Biol. **18:** 3604–3611.

Maduro, M., and D. Pilgrim, 1995 Identification and cloning of *unc-119*, a gene expressed in the *Caenorhabditis elegans* nervous system. Genetics **141:** 977–988.

Masselink, H., and R. Bernards, 2000 The adenovirus E1A binding protein BS69 is a corepressor of transcription through recruitment of N-CoR. Oncogene **19:** 1538–1546.

Mello, C. C., J. M. Kramer, D. Stinchcomb and V. Ambros, 1991 Efficient gene transfer in *C. elegans*: extrachromosomal maintenance and integration of transforming sequences. EMBO J. **10:** 3959–3970.

Miyabayashi, T., M. T. Palfreyman, A. E. Sluder, F. Slack and P. Sengupta, 1999 Expression and function of members of a divergent nuclear receptor family in *Caenorhabditis elegans*. Dev. Biol. **215:** 314–331.

Ozer, A., L. C. Wu and R. K. Bruick, 2005 The candidate tumor suppressor ING4 represses activation of the hypoxia inducible factor (HIF). Proc. Natl. Acad. Sci. USA **102:** 7481–7486.

Padilla, P. A., T. G. Nystul, R. A. Zager, A. C. Johnson and M. B. Roth, 2002 Dephosphorylation of cell cycle-regulated proteins correlates with anoxia-induced suspended animation in *Caenorhabditis elegans*. Mol. Biol. Cell **13:** 1473–1483.

Powell-Coffman, J. A., C. A. Bradfield and W. B. Wood, 1998 *Caenorhabditis elegans* orthologs of the aryl hydrocarbon receptor and its heterodimerization partner the aryl hydrocarbon receptor nuclear translocator. Proc. Natl. Acad. Sci. USA **95:** 2844–2849.

Praitis, V., E. Casey, D. Collar and J. Austin, 2001 Creation of low-copy integrated transgenic lines in *Caenorhabditis elegans*. Genetics **157:** 1217–1226.

Reinke, V., H. E. Smith, J. Nance, J. Wang, C. Van Doren *et al.*, 2000 A global profile of germline gene expression in *C. elegans*. Mol. Cell **6:** 605–616.

Ryan, H. E., J. Lo and R. S. Johnson, 1998 HIF-1 alpha is required for solid tumor formation and embryonic vascularization. EMBO J. **17:** 3005–3015.

Schofield, C. J., and P. J. Ratcliffe, 2005 Signalling hypoxia by HIF hydroxylases. Biochem. Biophys. Res. Commun. **338:** 617–626.

Semenza, G. L., 1999 Regulation of mammalian O2 homeostasis by hypoxia-inducible factor 1. Annu. Rev. Cell Dev. Biol. **15:** 551–578.

Semenza, G. L., 2000 HIF-1 and human disease: one highly involved factor. Genes Dev. **14:** 1983–1991.

Semenza, G., 2002 Signal transduction to hypoxia-inducible factor 1. Biochem. Pharmacol. **64:** 993–998.

Shen, C., D. Nettleton, M. Jiang, S. K. Kim and J. A. Powell-Coffman, 2005 Roles of the HIF-1 hypoxia-inducible factor during hypoxia response in *Caenorhabditis elegans*. J. Biol. Chem. **280:** 20580–20588.

Timmons, L., and A. Fire, 1998 Specific interference by ingested dsRNA. Nature **395:** 854.

To, K. K., and L. E. Huang, 2005 Suppression of hypoxia-inducible factor 1alpha (HIF-1alpha) transcriptional activity by the HIF prolyl hydroxylase EGLN1. J. Biol. Chem. **280:** 38102–38107.

Trent, C., N. Tsuing and H. R. Horvitz, 1983 Egg-laying defective mutants of the nematode *Caenorhabditis elegans*. Genetics **104:** 619–647.

Wang, G. L., B. H. Jiang, E. A. Rue and G. L. Semenza, 1995 Hypoxia-inducible factor 1 is a basic-helix-loop-helix-PAS heterodimer regulated by cellular O2 tension. Proc. Natl. Acad. Sci. USA **92:** 5510–5514.

Wenger, R. H., 2002 Cellular adaptation to hypoxia: O2-sensing protein hydroxylases, hypoxia-inducible transcription factors, and O2-regulated gene expression. FASEB J. **16:** 1151–1162.

Wicks, S. R., R. T. Yeh, W. R. Gish, R. H. Waterston and R. H. Plasterk, 2001 Rapid gene mapping in *Caenorhabditis elegans* using a high density polymorphism map. Nat. Genet. **28:** 160–164.

Yeo, E. J., Y. S. Chun and J. W. Park, 2004 New anticancer strategies targeting HIF-1. Biochem. Pharmacol. **68:** 1061–1069.

Communicating editor: K. Kemphues